

Energy shifts of $K\alpha$ x rays from highly stripped sulfur ions traveling in solids

R. L. Watson, A. Langenberg, R. A. Kenefick, C. C. Bahr, and J. R. White*

Cyclotron Institute, Texas A&M University, College Station, Texas 77843

(Received 5 December 1980)

The energies and intensities of the $2^3P_1 \rightarrow 1^1S_0$, and $2^1P_1 \rightarrow 1^1S_0$ transitions in He-like sulfur ions, and of the $2^2P \rightarrow 1^2S$ transition in H-like sulfur ions have been studied as a function of the thickness and electron density of the solid through which the ions travel. The thickness dependence of the x-ray intensities was analyzed in terms of a three-component model description of K -shell vacancy production and decay. Cross sections for electron excitation or ionization and capture deduced from this analysis were used to establish the energies of the x-ray peaks for complete emission in vacuum (i.e., outside the target). Energy shifts were obtained by comparing the peak energies for emission in thick targets to those for emission in vacuum. The results show that the energy shifts increase approximately linearly with the square root of the valence electron density of the target and are in good agreement with theoretical expectations.

I. INTRODUCTION

The passage of a highly stripped ion through a material medium causes a polarization of the loosely bound electrons of the medium encountered along its trajectory. In effect, these electrons act to screen the ion potential, thereby causing the core electron binding energies of the ion to decrease. As a result of this "dynamic screening" effect, the transition energies between electronic states of the ion inside the medium differ from those in vacuum.

Although such energy shifts have long been known to exist in high-density plasmas,¹ the first measurement in a solid was reported only recently by Bell *et al.*² These investigators measured the energy shift of the $2^1P_1 \rightarrow 1^1S_0$ transition in He-like sulfur ions traveling at 95 MeV in Al targets and obtained a value of -1.0 ± 0.2 eV. Using a simple perturbation argument, they showed that a shift of this magnitude is consistent with a dynamic screening constant given approximately by v/ω_p where v is the projectile velocity and ω_p is the plasma frequency of the target.

The concept of dynamic screening as it applies to this phenomenon originally evolved from the work of Lindhard³ and Brandt.⁴ Since the measurements of Bell *et al.*,² several theoretical works relating to dynamic screening have been published. Jakubassa⁵ has calculated the screened potential of an ion moving through a free-electron gas using linear-response theory and estimated the resulting decrease in the $2p$ - $1s$ transition energies. Crawford and Ritchie⁶ have studied the electronic states of swift channeled ions in terms of a time-dependent effective-Hamiltonian theory and calculated energies for low-lying states of hydrogenic ions channeled in Au. Tejada *et al.*⁷ have examined the energy shifts of two-electron states in swift ions passing through solids in a self-energy formulation.

Several aspects of this interesting problem remain to be explored experimentally. In particular, the dependence of the dynamic screening energy shift on the electron density of the target medium has not yet been established. In addition, the work of Jakubassa⁵ indicates that the energy shift should decrease as v^{-1} whereas the results of Crawford and Ritchie⁶ predict a v^{-2} dependence for channeled ions.

In the present study, measurements of the energy shifts for the $2^1P_1 \rightarrow 1^1S_0$ transition in He-like sulfur and for the $2^2P \rightarrow 1^2S$ transition in H-like sulfur were performed using a range of thick elemental targets whose average electron densities varied by about a factor of 20. A detailed examination of the target thickness dependence of the intensities and energy shifts in carbon targets was also carried out. This was necessitated by the presence of unresolved components near the transitions of interest.

II. EXPERIMENTAL METHODS

While in principle the problem of measuring x-ray energy shifts for heavy ions is straightforward, in practice several complications arise. First, in order to determine accurate absolute energies for x rays emitted from fast moving ions, Doppler-shift corrections must be applied. This requires a precise knowledge of the spectrometer observation angle. A second complication arises from the fact that other x-ray transitions may overlap with the ones of interest causing an apparent energy shift. A previous study has indicated that this is in fact the situation for 65-MeV sulfur ions.⁸

A beam of 65-MeV S^{4+} ions was extracted from the Texas A&M variable energy cyclotron, directed through a 3-mm-diameter collimator located 30 cm in front of the target position and focused on the target positioned at 45° with respect to the

beam axis. The beam alignment was established by the upstream collimator and a ZnS phosphor positioned 30 cm downstream from the target.

The spectra of $K\alpha$ x rays emitted by the sulfur ions over a 1-cm path length starting at the target surface were measured with a plane crystal spectrometer which had been mounted on a turntable, thus enabling it to be positioned at any observation angle between 162° and 20° with respect to the beam axis. The observation angle was established by a set of entrance soller slits having an angular divergence of 0.3° . The initial alignment of the system was accomplished by positioning the entrance soller slits perpendicular to the beam axis with the aid of a laser, to an estimated accuracy of $\pm 0.2^\circ$. Further details of the alignment procedure are given in Ref. 8.

Separate measurements were performed using a NaCl and a Ge Bragg crystal. The instrumental resolution for 2460-eV x rays was 6.9 eV full width at half maximum for the NaCl crystal and 10.2 eV FWHM for the Ge crystal. The spectrometer was calibrated during each run by measuring the spectra of S and Cl $K\alpha$ x rays from solid elemental sulfur (S_8) and KCl pellets excited either by 2.75-MeV protons or by 32-MeV oxygen ions. The oxygen ion induced spectra had previously been calibrated using the proton induced spectra.

As a check of the alignment, sulfur-ion spectra were measured at several angles using both the NaCl and Ge Bragg crystals. Measurements were performed at an observation angle of 161.5° , where the variation of the Doppler shift with angle is fairly small ($dE/d\theta \approx 0.8$ eV/deg), at 135.0° (where $dE/d\theta \approx 1.8$ eV/deg), and at 90.0° (where $dE/d\theta \approx 2.8$ eV/deg). The $K\alpha$ x-ray energies determined at all angles and with both crystals displayed an average root-mean-square deviation of 0.36 eV.

Most of the targets employed were metallic foils having thicknesses greater than the ranges of 65-MeV sulfur ions. Because of the uncertainties associated with determining the average projectile energies for x-ray emission in thick targets (see Ref. 9), the energy shift measurements were performed at an observation angle of 88.3° where the Doppler shift becomes almost independent of velocity in the energy range of 65–50 MeV.

Evidence for the existence of low-energy components in the peaks containing the $2^1P \rightarrow 1^1S$ and $2^2P \rightarrow 1^2S$ transitions was presented in Ref. 8. These components are believed to arise from the presence of a M -shell spectator electron. As a result, the desired energy shifts cannot be determined by simply subtracting the measured thick target peak energies from the theoretical energies for the $2^1P \rightarrow 1^1S$ and $2^2P \rightarrow 1^2S$ transitions in vacuum. Instead, it is necessary to establish experimentally

the apparent energies these composite peaks would have if they were observed in vacuum. This was accomplished by studying the dependence of the peak energies and intensities on target thickness using carbon foils. The carbon foils were self-supporting and were prepared by vacuum evaporation. They ranged in thickness from 5 to $300 \mu\text{g}/\text{cm}^2$. The thicknesses were determined by measuring the energy losses of 5.486-MeV alpha particles from an ^{241}Am source on passing through the foils. The x-ray peak intensities and energies were obtained by fitting the spectra with Voigt functions using the method of least squares. An example of a typical fitted spectrum is given in Ref. 8.

III. TARGET THICKNESS DEPENDENCE

The measured energy, \bar{E} , of an x-ray peak containing contributions from transitions taking place while the ion is inside the target as well as contributions from the same transitions occurring after the ion has emerged from the target (i.e., in vacuum) may be expressed in terms of the fraction of x-rays originating from outside the target f_0 ,

$$\bar{E} = f_0 \bar{E}_0 + (1 - f_0) \bar{E}_I, \quad (1)$$

where \bar{E}_0 is the average peak for emission outside the target and \bar{E}_I is the average peak energy for emission inside the target. Thus, an accurate determination of \bar{E}_0 requires a knowledge of f_0 as a function of target thickness. (The energy \bar{E}_I is obtained from a thick target measurement.)

A study of the thickness dependence of various x-ray lines excited in carbon targets was conducted for the purpose of deducing f_0 versus thickness for 65-MeV sulfur ions. The lines chosen for examination were the $(1s2p)2^3P_1 \rightarrow (1s^2)1^1S_0$, $(1s2p)2^1P_1 \rightarrow (1s^2)1^1S_0$, and $(2p)2^2P \rightarrow (1s)1^2S$ transitions. (These transitions will hereafter be referred to by their initial-state terms; 3P , 1P , and 2P .)

Spectra obtained for several carbon target thickness with the NaCl crystal are shown in Fig. 1. In the spectrum obtained with a $15 \mu\text{g}/\text{cm}^2$ target, the highest intensity peak arises from the 1P transition while the peak immediately to the left arises from the 3P transition. The 2P transition produces the highest intensity peak in the high-energy group around 2620 eV. (The energy scale in Fig. 1 has been adjusted to approximately remove the Doppler shift.) The rather dramatic decrease in the 3P intensity as the target thickness increases reflects the fact that the radiative lifetime of the 3P state is much longer than its collisional lifetime. Therefore, only 3P states which

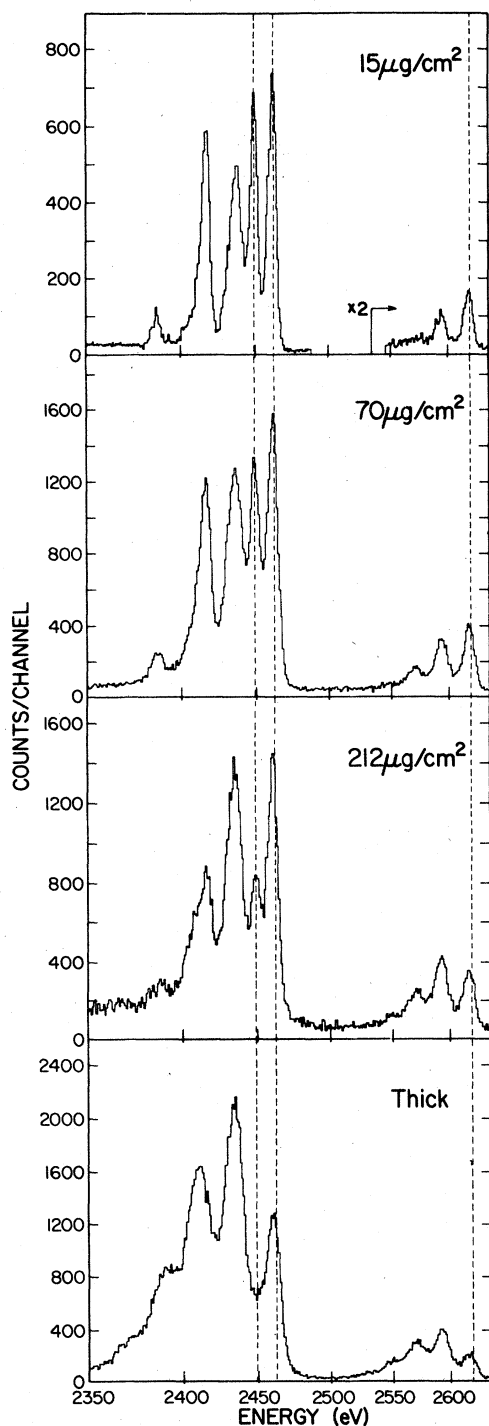


FIG. 1. Spectra of $K\alpha$ x rays from 65-MeV (incident energy) sulfur ions traveling through carbon targets of various thicknesses.

are populated near the back surface of the target and hence decay outside the foil are observed. Also, a considerable amount of line broadening is evident in the spectrum obtained with a thick

target. This broadening was studied earlier and attributed to collisional ionization and capture of K and L electrons.⁹

A quantitative description of the target thickness dependence of the fractions of the ion beam possessing zero, one, or two K vacancies has been given by Gardner *et al.*¹⁰ This treatment was based on the three-component model for the analysis of charge-changing collisions of H and He originally developed by Allison.¹¹ Consider the fraction of the ion beam Y_k , having k K -shell vacancies. The rate of change of this quantity with respect to depth in the target x (in units of atoms/cm²), is expressed by the differential equation

$$\frac{dY_k}{dx} = \sum_j \sigma_{jk} Y_j - Y_k \sum_j \sigma_{kj}, \quad (2)$$

where the σ_{kj} are cross sections for changing from k to j K -vacancies by ionization and excitation, or by electron capture and decay. In the case under consideration, $k = 0, 1, \text{ or } 2$, and three ionization plus excitation cross sections ($\sigma_{01}, \sigma_{02}, \sigma_{12}$) and three electron capture plus decay cross sections ($\sigma_{10}, \sigma_{20}, \sigma_{21}$) are involved. The various K -vacancy fractions are given by the following general solution to the coupled set of three equations resulting from Eq. (1) (Ref. 11)

$$Y_k(x) = Y_{k\infty} - f(q, k, x) e^{-0.5\sigma_T x} \quad (3)$$

where

$$\sigma_T = \sum_k \sum_{j \neq k} \sigma_{kj}$$

$Y_{k\infty} (= \lim_{x \rightarrow \infty} Y_k(x))$ is the equilibrium vacancy fraction and q is the number of K vacancies in the incident beam. The $Y_{k\infty}$ and $f(q, k, x)$ are complicated expressions involving the various σ_{kj} given in Ref. 11.

Extension of the above model to the description of the intensities of x-rays arising from particular excited states requires the following assumptions: (a) that the L -shell vacancy distribution reaches a statistical equilibrium much more quickly than does the K -shell vacancy distribution, and (b) that the L -shell vacancy distribution is independent of the number of K vacancies. The first assumption is quite reasonable in view of the large ionization cross sections for L electrons at these velocities. The second assumption is made plausible by the fact that in thick targets the $K\alpha$ x-ray satellite and hypersatellite relative intensity distributions are essentially identical.⁹ Proceeding on this basis then, the number of x rays per ion that originate from multiplet state J (having n L vacancies and k K vacancies) and escape through the front surface together with those emitted

after the ion has emerged from the foil may be expressed as^{9,12}

$$N_J = \omega_J G_J P_n [(nv\tau_J)^{-1} I_k + D_J F_k], \quad (4)$$

where ω_J is the fluorescence yield for state J (outside foil) and G_J is the probability that an ion having k K -shell and n L -shell vacancies will be in multiplet state J . P_n is the fraction of ions having n L -shell vacancies, n the number of target atoms/cm³, v the projectile velocity, τ_J the mean lifetime of state J and $I_k = \int_0^t Y_k(x) e^{-\sigma_a b x} dx$ where $Y_k(x)$ is the fraction of beam having k K -vacancies at depth x atoms/cm² [given by Eq. (3)]. $e^{-\sigma_a b x}$ is the absorption correction; σ_a is the x-ray absorption cross section and $b x$ is the path length; t is the target thickness (atoms/cm²); and $F_k = Y_k(t) e^{-\sigma_a b t}$.

$$D_J = \left[1 - \exp\left(-\frac{d}{v\tau_J}\right) \right],$$

where d is the path length for observing x-ray emission beyond the foil. The first term in Eq. (4) gives the contribution to the measured x-ray yield from emission inside the foil while the second term gives the contribution from emission outside the foil.

The object here is to use the measured thickness dependence of the 2P to 1P x-ray intensity ratio to deduce the set of cross sections required for Eq. (3). Then, the desired values of f_0 may be calculated from Eq. (4). Unfortunately, it is not possible to obtain a unique set of cross sections in this way without imposing certain restraints. Therefore, it was required that

$$\frac{\sigma_{02}}{\sigma_{01}} = \left(\frac{Y_2}{Y_1} \right)_{t \rightarrow 0},$$

$$\sigma_{01} = 3.3 \times 10^{-19} \text{ cm}^2.$$

The first condition is valid for single collisions (i.e., in the limit of zero target thickness). The second condition is based upon the cross section for single K -vacancy decay ($3.0 \times 10^{-19} \text{ cm}^2$) as calculated from the average lifetime for decay inside the foil ($1.4 \times 10^{-14} \text{ sec}$).¹³ The contribution to σ_{10} from electron capture was estimated to be $3 \times 10^{-20} \text{ cm}^2$ using the Oppenheimer-Brinkmann-Kramer formula given by Nikolaev (including screening).¹⁴ A reduction factor of 0.34, as indicated by the work of Chan and Eichler,¹⁵ was applied to obtain the above stated cross section. This cross section is a factor of 10 less than the contribution to σ_{10} from decay and hence it is not expected that error in the estimated electron-capture contribution will have a significant effect on the result.

Statistical population probabilities were used for

G_{2p} and G_{1p} and theoretical mean lifetimes for τ_{2p} ($2.44 \times 10^{-14} \text{ sec}$) (Ref. 16) and τ_{1p} ($1.49 \times 10^{-14} \text{ sec}$).¹⁷ Since the 2P and 1P states both have the same L -vacancy configuration, the P_n factors in Eq. (4) cancel in the ratio. Additional starting conditions were $\sigma_{12} = \frac{1}{2} \sigma_{01}$ and $\sigma_{21} = 2\sigma_{10}$. The best fit to the experimental 2P to 1P intensity ratios was obtained with the following set of cross sections:

$$\sigma_{01} = 2.8 \times 10^{-19} \text{ cm}^2,$$

$$\sigma_{12} = 0.8 \times 10^{-19} \text{ cm}^2,$$

$$\sigma_{02} = 0.07 \times 10^{-19} \text{ cm}^2,$$

$$\sigma_{21} = 6.0 \times 10^{-19} \text{ cm}^2,$$

$$\sigma_{10} = 3.3 \times 10^{-19} \text{ cm}^2,$$

$$\sigma_{20} = 0.01 \times 10^{-19} \text{ cm}^2.$$

It should be noted that, in a previous study of the yields of CuK x-rays produced by 64-MeV sulfur ions, Hopkins *et al.*¹⁸ obtained $Y_{1\infty} + 2Y_{2\infty} = 1$, whereas the set of cross sections deduced from the present data lead to a value of 0.6 for this quantity. The source of this discrepancy is not readily apparent. One possibility is that the estimated x-ray production cross section used by Hopkins *et al.*¹⁸ in their analysis was too small. Another possibility is that the G_{1p} and G_{2p} used in the present analysis deviate from those expected for a statistical population. In any case, calculations using a set of cross sections which satisfied the condition $Y_{1\infty} + 2Y_{2\infty} = 1$ (but did not give a good fit to the 2P to 1P intensity ratio data) yielded f_0 values which are not significantly different from those obtained with the set of "best-fit" cross sections given above.

The experimental thickness dependence of the 2P to 1P intensity ratio is compared with the representation obtained from Eq. (4) using the above cross sections (solid curve) in Fig. 2(a). The fit is quite good for thicknesses below $300 \mu\text{g}/\text{cm}^2$, but because the projectile energy dependence of the cross sections has not been taken into consideration, the calculation is not expected to give a good representation of the data at large target thicknesses. (The average beam energy in the target was taken to be 60 MeV in the above calculation.) The measured thickness dependence of the 3P to 1P intensity ratio is compared in Fig. 2(b) to that predicted by Eq. (4) using the same set of cross sections. As the thickness increases, the calculated curve drops below the data points. This is because the 3P peak contains overlapping contributions from several Li-like transitions which cannot be subtracted because they are unresolved.⁸ As the thickness increases, the Li-like transition

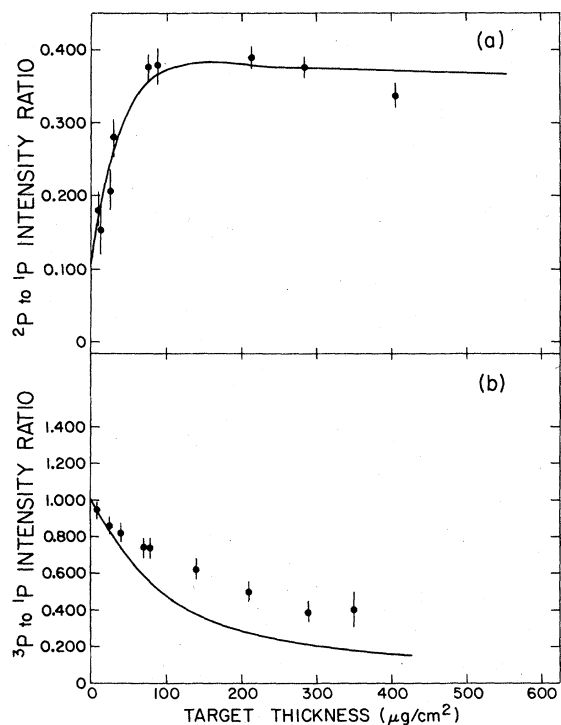


FIG. 2. (a) The ratio of the intensity of the H-like 2P transition to the intensity of the He-like 1P transition as a function of carbon-foil thickness. (b) The ratio of the intensity of the He-like 3P transition to the He-like 1P transition as a function of carbon-foil thickness. The solid curves show the results of the three-component model analysis.

intensities increase relative to the intensity of the 3P transition.

Having thus established values for the various cross sections required in the three-component model, it is now possible to calculate the relative numbers of x rays per ion which originate from inside and from outside the foil. The results of calculations for the 2P , 1P , and 3P transitions are shown in Fig. 3.

Returning now to the problem of determining the energies of the 1P and 2P peaks for total emission in vacuum, Fig. 4 shows the measured absolute energies of these peaks as a function of the carbon-foil thickness. The dashed line at the top of each portion of Fig. 4 indicates the theoretical energy for the pure transition taking place in vacuum (2461.4 eV for the $^2P \rightarrow 1^2S$ transition¹⁹ and 2621.7 eV for the $^2^2P \rightarrow 1^2S$ transition²⁰). The dashed line at the bottom of each portion of Fig. 4 indicates the measured peak energy for a thick carbon target in which all x-ray emission occurs inside the target (2457.8 \pm 0.3 eV for the 1P peak and 2617.4 \pm 0.5 eV for the 2P peak). Using the energy values measured for a 20 $\mu\text{g}/\text{cm}^2$ carbon target and the f_0 for this thickness as obtained

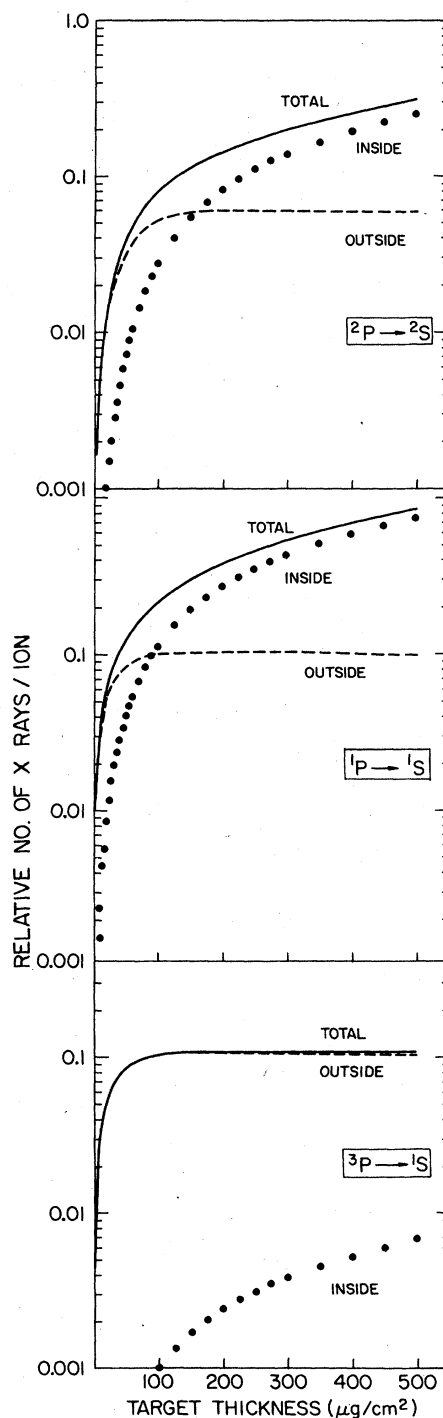


FIG. 3. The calculated relative yields of sulfur $K\alpha$ x rays originating from H-like 2P , and He-like 1P and 3P initial states, produced inside and outside of carbon targets as a result of the passage of 60-MeV sulfur ions.

from the three-component model calculation (Fig. 3), the average peak energies for emission in vacuum were calculated to be 2460.4 eV for the

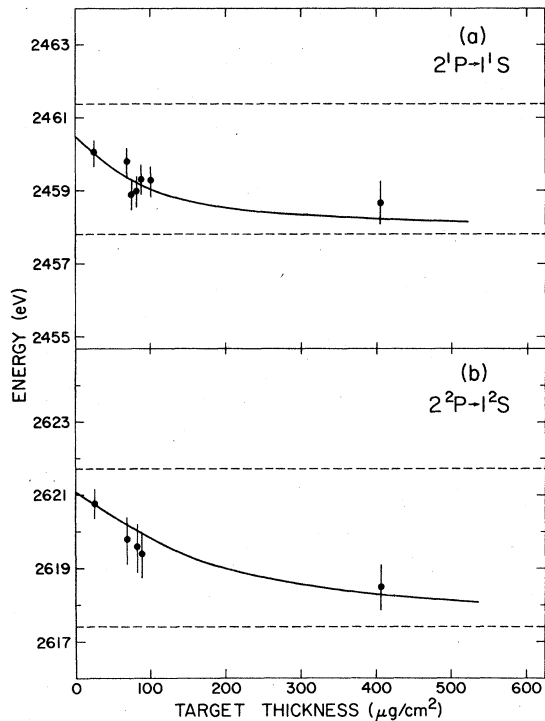


FIG. 4. The measured energies of the He-like $1P$ and H-like $2P$ x-ray peaks (corrected for Doppler shift) from 65-MeV (incident energy) sulfur ions as a function of carbon target-foil thickness. The upper dashed lines show the expected energies for pure transitions taking place in vacuum while the lower dashed lines show the measured peak energies for x-ray emission in thick targets. The solid curves show the results of the three-component model analysis.

$1P$ peak and 2621.0 eV for the $2P$ peak. The solid curves in Fig. 4 show the calculated dependences of these energies on target thickness.

IV. DEPENDENCE ON TARGET ELECTRON DENSITY

Having determined the energies of the $1P$ and $2P$ peaks for total emission in vacuum \bar{E}_0 , and mea-

sured their energies for total emission in solids \bar{E}_T , using a variety of thick targets, it is now possible to examine the dependence of the energy shift ($\bar{E}_0 - \bar{E}_T$) as a function of the electron density of the target. The results of these measurements are listed in Table I and shown in Fig. 5. In Fig. 5 the energy shifts for the 2^1P-1^1S and 2^2P-1^2S transitions are plotted versus the square root of the target valence electron density n_V . This latter quantity was calculated from the relationship

$$n_V = \frac{\rho N_A V}{W} \text{ (electrons/cm}^3\text{)}, \quad (5)$$

where ρ is the mass density (g/cm^3), N_A is Avogadro's number, V is the number of valence electrons, and W is the atomic weight.

To first order, the modification of the Coulomb potential acting on the core electrons of an ion traveling in a material medium caused by the polarization of the loosely bound electrons of the medium may be approximated by an exponential screening factor²¹ such that

$$V' = -\frac{Z'e^2}{r} e^{-r/d}, \quad (6)$$

where Z' is the effective nuclear charge of the ion and d is a screening constant characteristic of the medium. The change in the bound-state energy resulting from this additional screening is approximately

$$\Delta E \approx \Delta V = V - V' = -\frac{Z'e^2}{r} (1 - e^{-r/d}), \quad (7)$$

which for small r reduced to²

$$\Delta E \approx \frac{Z'e^2}{d}. \quad (8)$$

Thus, for a H-like ion, the first-order effect of the screening is to simply shift all energy levels up by the same amount leaving the transition energies between levels unchanged. For a He-like

TABLE I. Dynamic screening energy shifts for $K\alpha$ x rays from 65-MeV H-like and He-like sulfur ions.

Target	Valence electrons	Electron density ($10^{22}/\text{cm}^3$)	ΔE_{1P} (eV)	ΔE_{2P} (eV)
Li	1	4.7	0.4 ± 0.3	0.5 ± 0.3
Sb	5	16.6	1.8 ± 0.4	2.7 ± 1.3
Al	3	18.1	1.8 ± 0.8	2.9 ± 1.0
Si	4	20.0	2.1 ± 0.5	3.4 ± 1.0
Be	2	24.2	1.5 ± 0.3	1.7 ± 0.3
Cr	6	50.0	3.1 ± 1.0	3.7 ± 0.8
C	4	70.7	2.6 ± 0.5	3.6 ± 0.3
Co	9	82.0	3.6 ± 1.0	4.6 ± 1.0
Ni	10	91.4	3.1 ± 0.7	3.9 ± 0.5

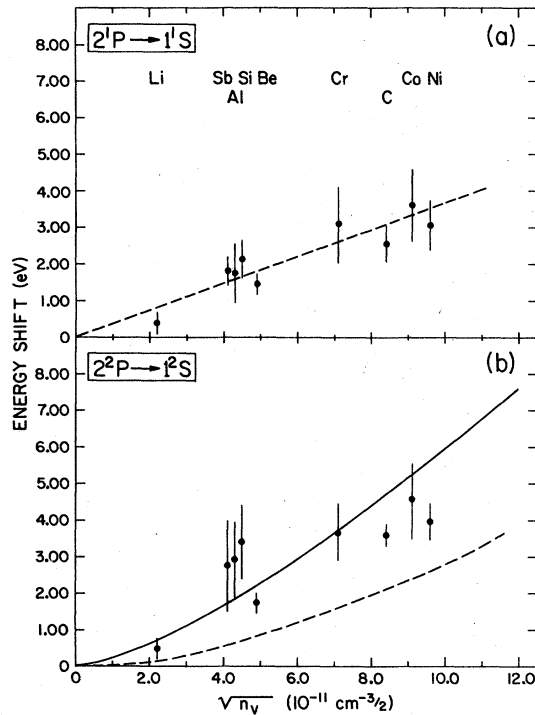


FIG. 5. (a) The energy shift of the He-like sulfur 2^1P transition as a function of the square root of the target valence electron density. The dashed line shows the shift given by Eq. (11). (b) The energy shift of the H-like sulfur 2^2P transition as a function of the square root of the target valence electron density. The dashed curve shows the scaled results of Rogers *et al.* (Ref. 22) while the solid curve shows the energy shifts predicted by the results of Jakubassa (Ref. 5).

ion, a first-order shift arises because the effective charge Z' is different for the initial and final states. Using Slater's screening rules, $Z'_{1s2p} = Z - 0.85$ and $Z'_{1s2} = Z - 0.30$; hence

$$\Delta E_{2p-1s} \approx \frac{0.55e^2}{d}. \quad (9)$$

If one uses a dynamic screening constant for d ,

$$d = \frac{2v}{\pi\omega_p}, \quad (10)$$

where v is the projectile velocity and ω_p is the plasma frequency of the target,³ the energy shift becomes

$$\Delta E_{2p-1s} = \frac{0.007\sqrt{n_v}}{v}, \quad (11)$$

in units of eV where n_v is in cm^{-3} and v is in cm/sec . The dashed line in Fig. 5(a) shows the energy shifts given by Eq. (11). The agreement with the experimental data is quite remarkable.

Rogers *et al.*²² have considered the problem of calculating the energy levels of a hydrogenic atom

in a screened Coulomb potential of the form given by Eq. (6). They obtained accurate numerical solutions to the Schrödinger equation for this potential and listed the eigenstate energies as a function of screening length. The dynamic screening energy shifts for hydrogenlike ions may therefore be estimated by taking the differences between $1s$ and $2p$ eigenstate energies for values of the screening length calculated from the dynamic screening constant Eq. (10). This procedure, which was suggested by Jakubassa,⁵ yields the dashed curve in Fig. 5(b). It is apparent that these estimates fall somewhat below the experimental data.

Jakubassa⁵ has calculated the energy shifts of electronic transitions of hydrogenlike ions caused by dynamic screening in the limit of high velocities (i.e., $v/v_F \gg 1$, where v_F is the Fermi velocity) using linear-response theory. A more complicated potential function involving a semiclassical expression for the dielectric constant is utilized in this treatment. The energy shift is obtained by first-order perturbation theory using unscreened hydrogenic wave functions. The result for transitions between the $2p(m = \pm 1)$ and $1s$ states is⁵

$$\Delta E_{2p-1s} \approx (4.52 \times 10^{-7}) \frac{n_v}{v^2} \left(8.25 \frac{v}{v_F} - 3 \ln \frac{v}{v_F} + 8.17 \right), \quad (12)$$

in units of eV where n_v is in cm^{-3} and v is in cm/sec . The solid curve in Fig. 5(b) shows the values of the energy shift given by Eq. (12). Considering the scatter of the experimental data, the agreement is quite good.

V. CONCLUSIONS

The energy shifts of $K\alpha$ x rays from 65-MeV H- and He-like sulfur ions traveling in a variety of solids have been determined for the purpose of investigating the dependence of dynamic screening on electron density. Because of the presence of unresolved components near the transitions of interest, it was necessary to carry out a detailed examination of the target thickness dependence of the 2^2P and 1^1P energies and intensities. A three-component model description of the development of K vacancies in the projectile as a function of depth in the target was extended to the analysis of the production and decay of specific excited states involving K vacancies, and provided a good representation of the observed intensity variations of the 3^3P , 1^1P , and 2^2P transitions. The electron excitation/ionization and capture cross sections deduced from this analysis were used to estimate the fractions of these x-ray intensities emitted from inside and outside of the targets. This in-

formation established the x-ray peak energies for complete emission outside the target and enabled the determination of energy shifts from absolute energies measured for thick targets.

It was found that the energy shifts increase approximately linearly with the square root of the valence electron density of the solid. Theoretical estimates based on a simple exponential screening approximation reproduced the data for the 2^1P-1^1S transition surprisingly well. A more sophisticated treatment of the screening in terms of linear-response theory yielded good

agreement with the data for the 2^2P-1^2S transition.

ACKNOWLEDGMENTS

The help of J. McCalpin, S. Merritt, D.A. Church, and J.F. Reading with the performance of the experiments and the interpretation of the results is gratefully acknowledged. This work was supported by the U.S. Department of Energy under Contract No. DE-AS05-78ER06036 and by the Robert A. Welch Foundation.

*Present address: U.S. Army Ballistics Research Laboratory, Aberdeen Proving Ground, Md. 21010.

¹H. R. Griem, *Spectral Line Broadening by Plasmas* (Academic, New York, 1974), pp. 146-153.

²F. Bell, H.-D. Betz, H. Panke, and W. Stehling, *J. Phys. B* **9**, L443 (1976).

³J. Lindhard, *K. Dan. Vidensk. Selsk. Mat.-Fys. Medd.* **28**, No. 8.

⁴W. Brandt, *Atomic Collisions in Solids* (Plenum, New York, 1975), Vol. 1, pp. 261-288.

⁵D. H. Jakubassa, *J. Phys. C* **10**, 4491 (1977).

⁶O. H. Crawford and R. H. Ritchie, *Phys. Rev. A* **20**, 1848 (1979).

⁷J. Tejada, P. M. Echenique, O. H. Crawford, and R. H. Ritchie, *Nucl. Instrum. Methods* **170**, 249 (1980).

⁸A. Langenberg, R. L. Watson, and J. R. White, *J. Phys. B* **13**, 4193 (1980).

⁹R. L. Watson, J. R. White, A. Langenberg, R. A. Kenefick, and C. C. Bahr, *Phys. Rev. A* **22**, 582 (1980).

¹⁰R. K. Gardner, T. J. Gray, P. Richard, C. Schmiedekamp, K. A. Jamison, and J. M. Hall, *Phys. Rev. A* **15**, 2202 (1977).

¹¹S. K. Allison, *Rev. Mod. Phys.* **30**, 1137 (1958).

¹²C. L. Cocke, S. L. Varghese, and B. Curnutte, *Phys. Rev. A* **15**, 854 (1977).

¹³H.-D. Betz, F. Bell, H. Panke, G. Kalkoffen, M. Wely, and D. Evers, *Phys. Rev. Lett.* **33**, 807 (1974).

¹⁴V. S. Nikolaev, *Zh. Eksp. Teor. Fiz.* **51**, 1263 (1966) [*Sov. Phys.—JETP* **24**, 847 (1967)].

¹⁵F. T. Chan and J. Eichler, *Phys. Rev. Lett.* **42**, 58 (1979).

¹⁶H. A. Bethe and E. E. Salpeter, *Quantum Mechanics of one- and two-Electron Atoms* (Springer, Berlin, 1958), p. 265.

¹⁷C. D. Lin, W. R. Johnson, and A. Dalgarno, *Phys. Rev. A* **15**, 154 (1977).

¹⁸F. Hopkins, J. Sokolov, and A. Little, *Phys. Rev. A* **15**, 588 (1977).

¹⁹G. W. F. Drake, *Phys. Rev. A* **19**, 1387 (1979).

²⁰J. D. Garcia and J. E. Mack, *J. Opt. Soc. Am.* **55**, 654 (1965).

²¹G. M. Harris, *Phys. Rev.* **125**, 1131 (1962).

²²F. J. Rogers, H. C. Graboske, Jr., and J. D. Hardwood, *Phys. Rev. A* **1**, 1577 (1970).